Evaluating the Importance of Rear Spoiler on Energy Efficiency of Electric Vehicles

S. M. R. Tousi[1,*], P. Bayat[2], P. Bayat[3]

1 Assistant Professor, Department of Electrical Engineering, Faculty of Engineering, Bu-Ali Sina University, Hamedan, Iran 2,3 Ph.D. Student, Department of Electrical Engineering, Faculty of Engineering, University of Guilan, Rasht, Iran

tousi@basu.ac.ir

Abstract

Electric vehicles (EVs) have gained the attention of many authorities, automakers and researchers due to their considerable energy saving and emission reduction. One of the main issues that must be considered in design of a road vehicle is the calculation of aerodynamic forces. This issue also must be scrutinized in the design of EVs. Installation of rear spoiler is one of the solutions proposed for reduction of aerodynamic drag in racing cars and consequently increasing their maximum speed. This study focuses on the effects of installing a rear spoiler on an EV. The vehicle's drag and lift coefficients are determined by solving a 3D steady-state incompressible solution of Navier-Stokes equations with computational fluid dynamic (CFD) analysis in ANSYS FLUENT. In order to verify the effects of installing a rear spoiler on an EV, all the components were modelled in MATLAB /SIMULINK also, practical tests were performed to confirm and verify the simulation results. The results show that installing a rear spoiler on an EV, not only improves the aerodynamic characteristics of vehicle but also improves operating efficiency of electric motor and some operational aspects of batteries. In addition, it is shown that an EV with a rear spoiler is able to travel more in comparison with an EV without rear spoiler.

Keywords*: Electric Vehicle; Rear Spoiler; Aerodynamic Forces; Energy Efficiency.*

1. Introduction

Cars with Internal Combustion Engine (ICE) are the major sources of urban pollution. In addition, they are extremely inefficient in utilizing the energy of fossil fuel. Hence, the problems associated with ICE automobiles include environmental, economical, as well as political issues [1]. These concerns have forced governments all over the world to consider alternative vehicle concepts. The EV was conceived in the middle of previous century as the most promising solution for reducing the emission while increasing the efficiency. EVs have been widely studied and major improvements have been achieved during the last decade. More recent works have been focused on energy storage systems (ESS) and power electronic devices.

Vehicle aerodynamics plays a significant role in the design, safety and efficiency of all vehicles. Any improvement in aerodynamic characteristics can result in significant changes in driving stability, handling, energy consumption and overall efficiency of vehicle. Rear spoiler is one of the solutions proposed for this purpose. It is relatively inexpensive, easy to install and aesthetically appealing. Furthermore, it can reduce the lift and drag coefficients and increase the energy efficiency significantly for most of the passenger vehicles [2-5]. In addition, a better traction, turning, acceleration and brake performance can be achieved by installing the rear spoiler. It must be noted that installation of rear spoiler might make the aerodynamics of a vehicle worse in case of not considering design and aerodynamics rules.

Even though the rear spoiler plays a relatively important role in aerodynamics of vehicles, there are only limited numbers of reported studies in which both the computational analysis and experimental analysis have been provided. In addition, all of them have only focused on ICE or pure fuel cell vehicles. These studies deal with different types of vehicles ranging from small mini-vans to modified race cars. Improving aerodynamic and aero-acoustic characteristics, preventing exhaust smoke patterns and even reducing the snow accumulating on the rear

surface of the vehicle are some outcomes of rear spoiler reported in these researches [6, 7].

Zake in [2] investigated the effects of rear spoiler on car aerodynamics drag and stability. His researches showed that the rear spoiler can reduce the drag by creating high pressure at the back of vehicle. In order to enhance the efficiency of vehicle, authors in [3] used rear spoiler for decreasing the drag and lift forces and increasing the cross-wind stability of the vehicle. In [4], two different types of simulations were made on the flow around a simplified high speed passenger car with and without a rear-spoiler. Results showed that a mild reduction of the vehicle aerodynamics drag leads to less vehicle fuel consumption on the road. According to numerical simulations in [5], the aerodynamic drag and lift on a low mass vehicle moving at 30 m/s reduce more than 5 % with installation of proposed spoiler.

Takemori et al. in [8] performed wake control experiments for a bluff-based bus-like body model by installing air guide vanes at the based rear and corners in order to reduce the aerodynamic drag. Authors in [9] showed that the aerodynamic drag of the commercial bus can be reduced by 16% with the use of a rear spoiler. The authors used FLUENT as the CFD solver with k-ε model. Mason et al. in [10] performed wind tunnel test to investigate the effect of fairings on drag forces. The effects of air deflector in trucks have been also investigated by Fujimoto et al. in [11]. Garry in [12] performed experiments on the container-mounted devices for reducing the aerodynamic drag of commercial vehicles. In addition, many authors have used CFD techniques for numerical simulations of automobile [13–17].

So, it seems that there is no reported research on analyzing the effects of installing rear spoilers on EVs. The performance aspects that need to be investigated include items such as traveling distance or electrical range, battery usage, battery health and overall EV efficiency and performance. The current study aims at presenting the effects of rear spoiler installation on an EV through simulations and practical tests.

The remainder of this paper has been organized as follows: The physical description and numerical modeling are discussed in section 2. In section 3, the EV is modeled. The performances of EV with spoiler and without spoiler are compared and discussed through simulations in section 4. Practical tests are presented in section 5. Finally, concluding remarks are presented in section 6.

2. Governing equations and turbulent modeling

The numerical solution of any fluid flow problem requires the solution of the general equations of fluid motion, the Niver-Stocks and the continuity equations. Fluid flow problems are described mathematically by equations (1) to (3) which are a set of coupled non-linear partial differential equations with appropriate boundary conditions. These equations are derived from Newton's Second Law and describe the conservation of momentum in the flow [18].

The general from of the three dimensional incompressible instantaneous Navier-Stokes equations in Cartesian tensor from are as follow:

$$Acceleration\ term = convection\ term - pressure\ gradient + effects\ of\ viscosity + body\ force$$

Therefore:

$$\frac{\partial(\rho u_i)}{\partial t} = -\frac{\partial(\rho u_i u_j)}{\partial x_j} - \frac{\partial P}{\partial x_i} + \frac{\partial}{\partial x_j}\left[\mu\left(\frac{\partial u_i}{\partial x_j} + \frac{\partial u_j}{\partial x_i}\right)\right] + F, \quad i,j = 1,2,3; \tag{2}$$

And the continuity equation:

$$\frac{\partial \rho}{\partial t} + \frac{\partial \rho u_i}{\partial x_i} = 0 \qquad i = 1,2,3; \tag{3}$$

In order to consider the turbulence effect on the flow field, Reynolds time averaging technique was employed on the Navier-Stokes equation to yield the Reynolds averaged Navier-Stokes equation. The $k-\varepsilon$ model is the most common model used in CFD to simulate mean flow characteristics in turbulent flow conditions. The turbulence model used in this work is the standard $k-\varepsilon$ turbulence model because of its good prediction of complex flows [19]. The standard $k-\varepsilon$ model has two model transport equations; one for the turbulent kinetic energy of the flow, k, and one for the dissipation rate of k, ε. These values are used to define the velocity scale and length scale at any given point and time in the flow field, representative of large scale turbulence.

Velocity scale: $\vartheta = k^{\frac{1}{2}}$ (4)

Length scale: $l = \frac{k^{\frac{3}{2}}}{\varepsilon}$ (5)

Eddy viscosity can be specified as follows:

$$\mu_t = C_\mu . l . \vartheta = \rho C_\mu k^2/\varepsilon \tag{6}$$

Inserting the Boussinesq hypothesis into the momentum equation yields [20]:

$$\frac{\partial(\rho\bar{u}_i)}{\partial t} = -\frac{\partial\left(\rho\bar{u}_i\bar{u}_j\right)}{\partial x_j} - \frac{\partial\bar{P}}{\partial x_i} + \frac{\partial}{\partial x_j}\left[(\mu+\mu_t)\left(\frac{\partial\bar{u}_i}{\partial x_j} + \frac{\partial\bar{u}_j}{\partial x_i}\right)\right] \quad , \quad i,j = 1,2,3 \tag{7}$$

The complete formulation of the standard $k-\varepsilon$ model equation is given in Einstein summation convention as follows:

Turbulent kinetic energy:

$$\rho\frac{\partial k}{\partial t} + \rho\bar{u}_j\frac{\partial k}{\partial x_j} = \tau_{ij}\frac{\partial\bar{u}_i}{\partial x_j} - \rho\varepsilon + \frac{\partial}{\partial x_j}\left[\left(\mu+\frac{\mu_t}{\sigma_k}\right)\frac{\partial k}{\partial x_j}\right] \quad , \quad i,j = 1,2,3 \tag{8}$$

Dissipation rate:

$$\rho\frac{\partial\varepsilon}{\partial t} + \rho\bar{u}_j\frac{\partial\varepsilon}{\partial x_j} = C_{\varepsilon1}\frac{\varepsilon}{k}\tau_{ij}\frac{\partial\bar{u}_i}{\partial x_j} - C_{\varepsilon2}\rho\frac{\varepsilon^2}{k} + \frac{\partial}{\partial x_i}\left[\left(\mu+\frac{\mu_t}{\sigma_\varepsilon}\right)\frac{\partial\varepsilon}{\partial x_j}\right] \quad , \quad i,j = 1,2,3 \tag{9}$$

Where

$$\tau_{ij} = 2\mu_t S_{ij} - \frac{2}{3}\rho k\delta_{ij} = Reynolds\ stress\ tensor \tag{10}$$

$$\delta_{ij} = the\ Kronecker\ delta\ (1\ when\ i=j) \tag{11}$$

$$S_{ij} = \left(\frac{\partial\bar{u}_i}{\partial x_j} + \frac{\partial\bar{u}_j}{\partial x_i}\right) \tag{12}$$

The coefficients of model are modified based on [21] such that $C_{\varepsilon1} = 1.44, C_{\varepsilon2} = 1.92, \sigma_\varepsilon = 1.3, \sigma_k = 1, C_\mu = 0.09$. These default values have been determined from experiments with water and air for fundamental turbulent shear flows including homogeneous shear flows and decaying isotropic grid turbulence.

After 3500 iterations done in ANSYS FLUENT, the drag coefficient without the spoiler was calculated to be 0.404. When the spoiler was added, the drag coefficient decreased to 0.378. In addition, the lift

A 3D steady state, incompressible solution of the Navier-Stokes equations was performed using ANSYS FLUENT® in order to determine the vehicle's drag and lift coefficients. Turbulence modeling was done with the realizable k-ε model using non- equilibrium wall functions. Results for a vehicle with spoiler and without spoiler were obtained with the same meshing resolutions (see appendix I), the same k −ε turbulence model, and also the same boundary conditions. The free stream velocity was set to be 25m/s.

In order to study the effect of spoiler installation on aerodynamics, drag and lift coefficients of a vehicle, one spoiler modeled as shown in Figs. 1 and 2. It also was analyzed in XFLR5 software. This spoiler has 4.6 ft. length and 1.2 ft. width.

The pressures around the vehicle without spoiler and with spoiler are shown in Figs. 3 and 4. There are two additional contributions to the total pressure force on the vehicle with the spoiler when compared with that on the vehicle without the spoiler. The first contribution is made by the net pressure force on the spoiler which is the major contribution to the lift reduction, and the second contribution is due to the increase in pressure on the back surface of the vehicle due to the diffuser effect of the spoiler which is the major contribution to the drag reduction coefficient decreased from 0.008 to -0.036. Fig. 5 shows drag and lift coefficients with and without spoiler.

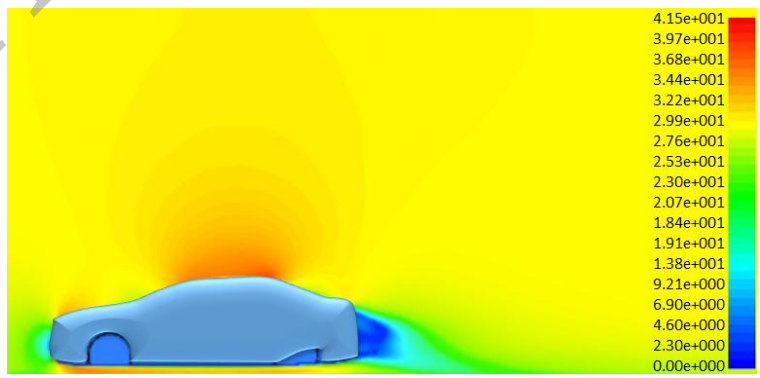

Fig. 3. Pressure around the vehicle without the spoiler

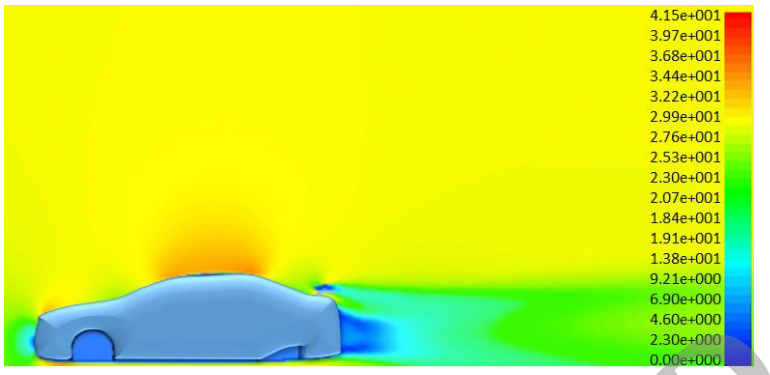

Fig. 4. Pressure around the vehicle with the spoiler

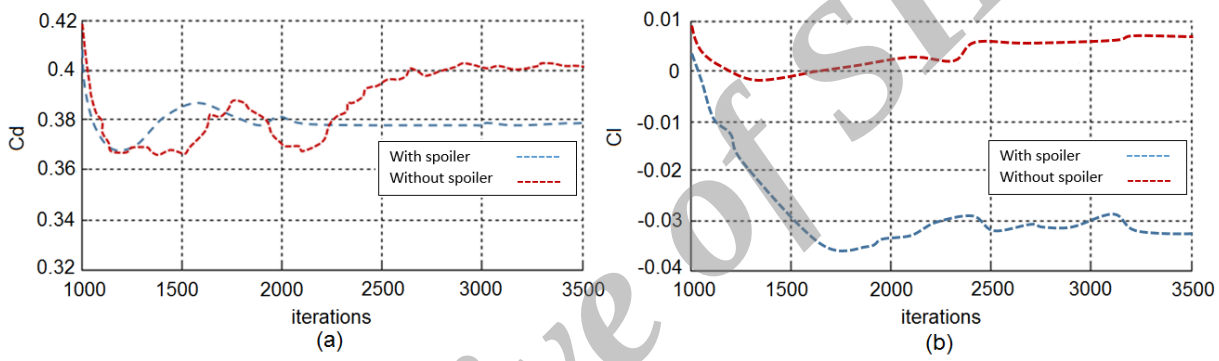

Fig.5. (a) Drag coefficient with and without rear spoiler, (b) Lift coefficient with and without rear spoiler

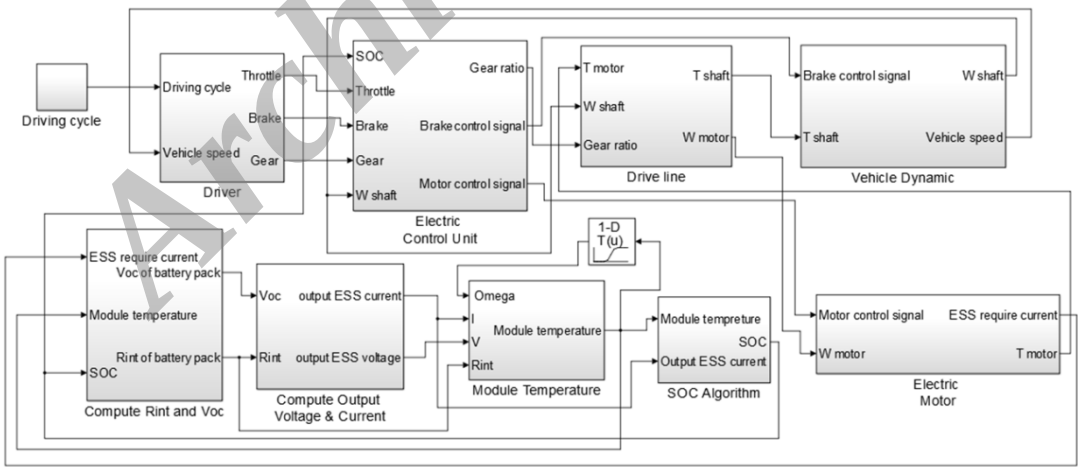

Fig 6. Electric vehicle model in SIMULINK

3. System configuration

In order to determine the effects of rear spoiler on the performance of EV, necessary blocks including driveline, controller, electric motor, energy storage system (battery, DC/DC converter, etc.) and vehicle dynamics were modeled as shown in Fig.6. The requested speed given by accelerator pedal position is the input of the system while the motor torque and speed are the outputs of the system. In the following, each block is explained in more detail. Table I provides specifications of the electric vehicle which

was used in simulations [22]. This vehicle has been built by our team and currently is under development (see Fig. 7).

Fig. 7. Proposed EV

Table I. Specifications of the electric vehicle

Total weight	450 kg
Vehicle length	4100 mm
Vehicle width	1700 mm
Vehicle height	1400 mm
Centre of mass height from ground	0.45 m
Horizontal distance of center of mass from front axle	1.35 m
Horizontal distance of center of mass from rear axle	1.25 m
Coefficient of rolling resistance	0.011
Drag coefficient	0.378 (with spoiler) 0.404 (without spoiler)
Lift coefficient	-0.036 (with spoiler) 0.008 (without spoiler)
Frontal area	2.7 m^2
Rolling radius of tire	0.32 m
Final drive ratio	5.21
Transmission efficiency	96% (assumed constant through all gears)
Inertia of electric engine	0.31 $kg.m^2$
Inertia of wheel and axle	1.2 $kg.m^2$
Battery max discharge current	150 Amps
Supercapacitor max discharge current	200 Amps

3.1 Vehicle dynamics and Motion Equations

The traction force of a vehicle, can be described by following equations [23]:

$$F_{total} = Inertial\ force\ (F_I) + Gravitational\ force\ (F_G) + Rolling\ resistance\ force\ of\ the\ wheels\ (F_{rr}) + Aerodynamic\ forces\ due\ to\ wind\ resistance \begin{pmatrix} drag\ force\ (F_d) \\ and\ lift\ force\ (F_L \end{pmatrix}$$

Where:

$$F_I = M_v.\dot{V}_v \quad (14)$$

$$F_G = M_v.g.\sin(\alpha) \quad (15)$$

$$F_{rr} = M_v.g.\cos(\alpha).sign(V_v).C_{trr} \quad where \quad C_{trr} = [100 + 3.6V_v].10^{-4} \quad (16)$$

$$F_d = \frac{1}{2}.c_d.\rho_a.A_f.(V_v + V_w)^2 \quad (17)$$

$$F_l = \frac{1}{2}.c_d.\rho_l.A_f.(V_v + V_w)^2 \quad (18)$$

Fig. 8 shows the forces acting on a vehicle

Longitudinal and lateral velocities and yaw rate are given by the following equations [24, 25]:

$$\dot{v_x} = r.v_y + \frac{1}{M_v}\big[(F_{xfl} + F_{xfr}).\cos(\delta_f) - (F_{yfl} + F_{yfr}).\sin(\delta_f) + F_{xrl} + F_{xrr}\big] \quad (19)$$

$$\dot{v_y} = -r.v_x + \frac{1}{M_v}\big[(F_{xfl} + F_{xfr}).\sin(\delta_f) + (F_{yfl} + F_{yfr}).\cos(\delta_f) + F_{yrl} + F_{yrr}\big] \quad (20)$$

$$\dot{r} = \frac{1}{I_z}\Big[L_f(F_{xfl} + F_{xfr}).sin(\delta_f) + L_f(F_{yfl} + F_{yfr}).\cos(\delta_f) - L_r(F_{yrl} + F_{yrr}) - \frac{T_f}{2}(F_{xfl} - F_{xfr}).\cos(\delta_f) + \frac{T_f}{2}(F_{yfl} + F_{yfr}).\sin(\delta_f) - \frac{T_r}{2}(F_{xrl} - F_{xrr})\Big] \quad (21)$$

Where F_{xfl}, F_{xfr}, F_{xrr}, F_{xrl}, F_{yfl}, F_{yfr}, F_{yrr} and F_{yrl} are longitudinal and lateral tire forces. Fig. 9 shows these forces acting on a vehicle.

3.2 Battery Model

Lithium-ion batteries are now generally accepted as the best choice for energy storage in electric vehicles. This superiority lies on its better power and energy density in comparison with lead-acid or nickel-metal-hydride batteries [26]. The battery model used in this paper is based on a high-power lithium ion cell [27], which provides high power density and high efficiency.

Battery characteristics are determined by internal chemical reactions. These reactions are affected by the ambient temperature, the state of charge (SOC), the charge–discharge rate and charge–discharge history. Battery characteristics cause substantial issues in battery management. The battery characteristics can be modeled as following:

$$P_b = P_s + P_{loss}(P_s, E_s, T) \quad (22)$$

The battery energy level is given by (23).

$$E_s(t) = E_s(0) + \int_0^t P_s(\tau)\, d\tau \quad (23)$$

It is not easy to predict the charge/discharge current and SOC variations of battery. The current flowing into the battery is determined based on the charging voltage and the internal impedance of the battery [28]. As illustrated in [29], SOC can be estimated by offline or online methods. In offline methods, the battery needs to be charged and discharged in a specific direction in order to extract its features from the acquired data. Offline methods usually given proper estimation of battery SOC, however they are time consuming, expensive and also interrupt battery operation. Therefore, researchers are generally interested in methods with online estimation of SOC [30, 31]. The most common method of SOC calculation that also has been selected in this study is Coulomb-counting. The equations are as follow.

$$SOC = SOC_0 + \frac{1}{C_n}\int_{t_0}^{t}|I|dt \quad \text{During} \quad (24)$$

Charging

$$SOC = SOC_0 - \frac{1}{C_n}\int_{0}^{t}|I|dt \quad \text{During} \quad (25)$$

Discharging

However, this method needs an accurate measurement of battery current and also knowing the initial value of SOC (SOC0).

The dynamic model of battery is presented in Fig. 10. It should be noted that the battery open circuit voltage and lumped resistance R_i are strongly dependent on battery SOC and module temperature. According to Fig. 10, current of battery pack is calculated as following equation:

$$I_b = \frac{V_{oc} \pm \sqrt{{V_{oc}}^2 - 4P_rR_{int}}}{2R_{int}} \quad (26)$$

There are a lot of stressful conditions such as high power draw and severe ripple current in high acceleration and speed for an EV's battery. These issues may lead to thermal runaway of some cells and propagation of excessive temperature throughout a battery pack. The main problem caused by temperature is decreasing of the battery performance. Therefore, a thermal management system must prevent such a propagation. So, it is necessary to analyze the battery thermal behavior and thermal management effect. In order to determine the effect of spoiler on EV battery pack temperature, the lumped capacitance battery thermal model which initially developed by Steve Burch [32] at National Renewable Energy Laboratory (NREL) has been used. The governing formulas as explained in [33] are as follow. Fig. 11 shows the configuration of battery thermal design and analysis.

$$H_d = \frac{T_{ess} - T_{air}}{R_{eff}} \quad (27)$$

$$R_{eff} = \frac{1}{h\gamma} + \frac{t}{k\gamma} \quad (28)$$

$$h = \begin{cases} a\left(\frac{m/\rho A}{5}\right)^b & T_{ess} > T_{ess-set} \\ 4 & T_{ess} > T_{ess-set} \end{cases} \quad (29)$$

$$T_S = T_{amb} + \frac{0.5H_d}{r_{air}C_{p,air}} \quad (30)$$

$$p_{l,ess} = \eta_c R_{int} I^2 \quad (31)$$

$$T_{ess} = \int_0^t \frac{H_d - L_{ess}}{m_{Batt}C_{p,Batt}}\, dt \quad (32)$$

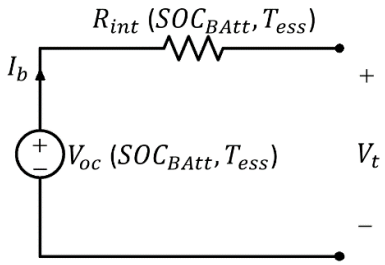

Fig. 10. Dynamic model of battery

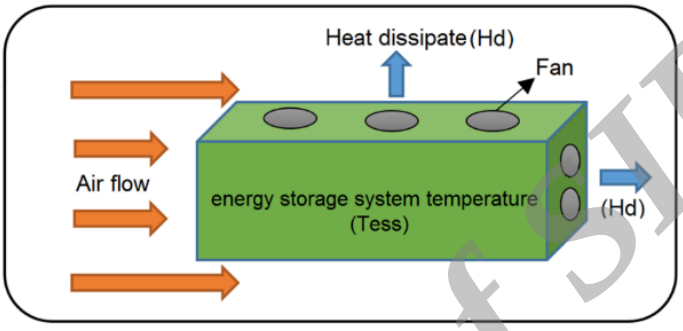

Fig. 11. Configuration of the battery thermal analysis

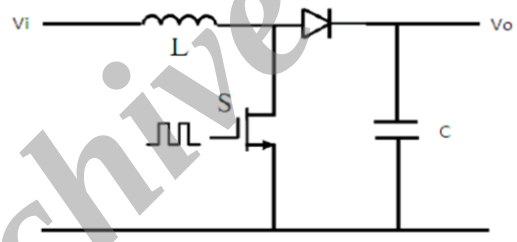

Fig 12. Configuration of boost regulator

3.3 DC/DC converter model

The electric system also contains a DC/DC converter. The role of the DC/DC converter is converting the battery voltage to a proper level in order to be feed to the electric motor. This electric motor has been assumed a Brushless DC motor (BLDC). In this paper a boost converter has been used based on load voltage and impedance matching requirements (see Fig.12). In a boost convertor, output voltage is larger than input voltage and they are related by the following equation [34].

$$V_o = \frac{1}{1-D} V_i \qquad (33)$$

3.4 Electric motor model

In this study a permanent magnet brushless DC motor has been selected for moving the EV [35]. The motor efficiency is a function of motor torque (T_m) and speed (w_m) as shown in Fig. 13. Since, the battery power and motor torque have operational limits, the final motor torque becomes:

$$T_m = \begin{cases} \min\left(T_{m,r}, T_{m,d}(\omega_m), T_{batt,d}(SOC, \omega_m)\right) & if\ T_{m,r} \\ max\left(T_{m,r}, T_{m,c}(\omega_m), T_{batt,c}(SOC, \omega_m)\right) & if\ T_{m,} \end{cases}$$

3.5 Driveline model

The set of transmission elements and the propulsion unit are referred to as the drivetrain of the vehicle. The transmission is a mechanical linkage that transmits power between the electric motor shaft and

the wheels [36, 37]. The drivetrain is also known as powertrain of the vehicle. The static models have been used for modeling of driveline components (equations (35) to (38)). The drivetrain of an EV consists of the electric motor, gearbox, driveshaft, differential, half-shaft and wheels. In addition, a discrete-time dynamic system was used for gear-shifting sequence.

$$T_{tr} = \eta_{tr}(g_n).R_{tr}(g_n).\left(T_t - T_{tr,loss}(\omega_t, g_n)\right) \quad (35)$$

$$T_{df} = \eta_{df}.R_{df}.\left(T_{tr} + R_c.\eta_c.T_m - T_{df,loss}(\omega_t)\right) \quad (36)$$

$$T_p = \frac{T_t}{T_r(w_{rc})} = \left(\frac{\omega_e}{K(w_{rc})}\right)^2 \ , \ \omega_{rc} = \frac{\omega_t}{\omega_e} \quad (37)$$

$$g_n(k+1) = \begin{cases} 1, & g_n(k) + S(k) < 1 \\ g_n(k), & 1 < g_n(k) + S(k) < 4 \\ 4, & g_n(k) + S(k) > 4 \end{cases} \quad (38)$$

4. Simulation results and discussion

In order to verify the effects of installing a rear spoiler on an EV, all the components were modeled in MATLAB /SIMULINK. Then, the performance of EV was investigated through simulation in case of an Urban Dynamometer Driving Schedule (UDDS) [38]. Fig. 14 shows the UDDS driving cycle.

Researches show that in a typical ICE car and at the speed of 100 km/h, aerodynamic drag force consumes about 65% of the total energy [39, 40]. Simulations showed that rear spoiler reduced the drag coefficient about 7% (from 0.404 to 0.378). In addition it led to decreasing the lift coefficient from 0.008 to -0.036. Fig.15 shows the drag powers obtained at different speeds of UDDS in two cases of installing rear spoiler and without it. This reduction definitely results in reduction of energy consumption in regular vehicles and EVs, but in EVs this reduction has some more benefits that will be addressed later.

In order to understand the importance of lift coefficient reduction due to installation of rear spoiler on EVs, the effects of the lift coefficient on the rolling resistance and slip angles has been assessed. If the tire moves with a slip angle, as it is the case any time it exerts a side force F_y (see Fig. 9), a strong increase of rolling resistance can be expected [41].

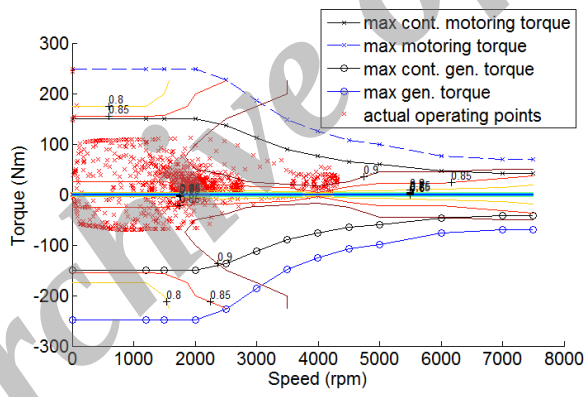

Fig. 13. Efficiency map of the electric motor

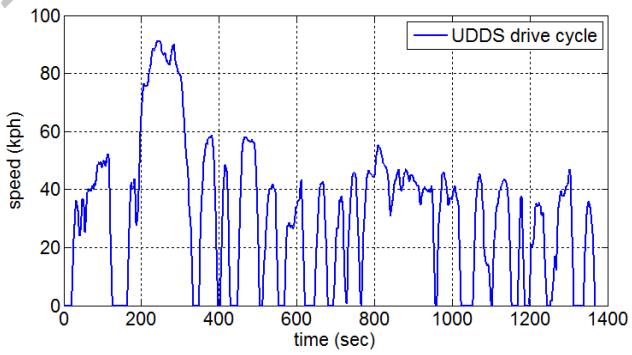

Fig. 14. Requested vehicle speed in UDDS driving cycle

According to Fig. 9, the longitudinal slip for front and rear tires is defined as the relative difference between a driven wheel angular velocity and the vehicle velocity [42] which can be expressed as:

$$\sigma_f = \begin{cases} \frac{w_f R_f - V_v}{w_f R_f} & w_f R_f > V_v, w_f \neq 0 \quad for \text{ acceleration} \\ \frac{w_f R_f - V_v}{v_x} & w_f R_f < V_v, V_v \neq 0 \quad for\ braking \end{cases} \tag{39}$$

$$\sigma_r = \begin{cases} \frac{w_r R_r - V_v}{w_r R_r} & w_r R_r > V_v, w_f \neq 0 \quad for \text{ acceleration} \\ \frac{w_r R_r - V_v}{V_v} & w_r R_r < V_v, V_v \neq 0 \quad for\ braking \end{cases} \tag{40}$$

According to simulation results shown in Fig. 16, installing spoiler reduces wheel slip of drive wheels. Furthermore, the rolling resistance decreases and consequently less energy is being consumed for traction force.

Another issue that can be investigated after installing rear spoiler for an EV is battery health status. Battery health management plays a vital role in defining the State of Health (SOH) of battery based on different aging processes. Rezvanizaniani et al. in [43] provided a review of battery Prognostics and Health Management (PHM) techniques. Any parameter that changes considerably during operation such as internal resistance and capacity can be used as an indicator of battery SOH. Rapid loss of power and sudden rise of temperature are some examples of events that reduce the battery life, but engine has to produce more power in order to overcome the force of air resistance and consequently more current should be drawn from the battery. It is clear that by reducing the air resistance and aerodynamic drag, this problem can be solved. Therefore, in order to improve the performance of the battery module, installing a rear spoiler is a feasible and perfect solution. Figs. 17 and 18 apparently show the effect of rear spoiler on battery current and temperature respectively. The reduction of battery temperature in turn increases the battery life. Furthermore, as illustrated in Fig. 19, the higher amount of current drawn from the battery also leads to increment in actual power loss in the ESS. Therefore, as can be seen from Fig. 20 the value of SOC with and without spoiler at the same amount of battery charge are different.

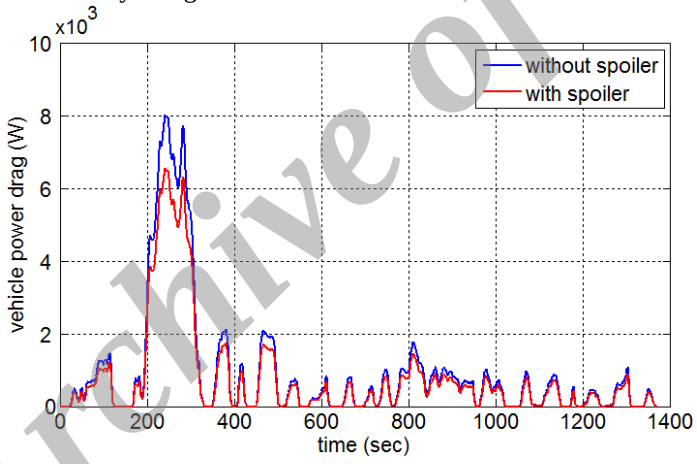

Fig. 15. Vehicle power drag at different vehicle speeds

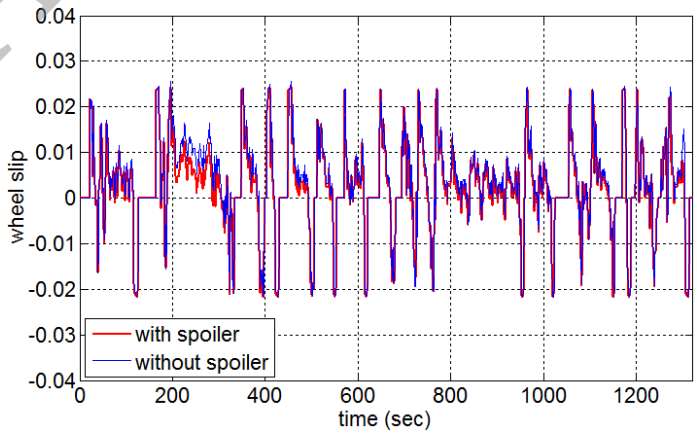

Fig. 16. Wheel slip of drive wheel

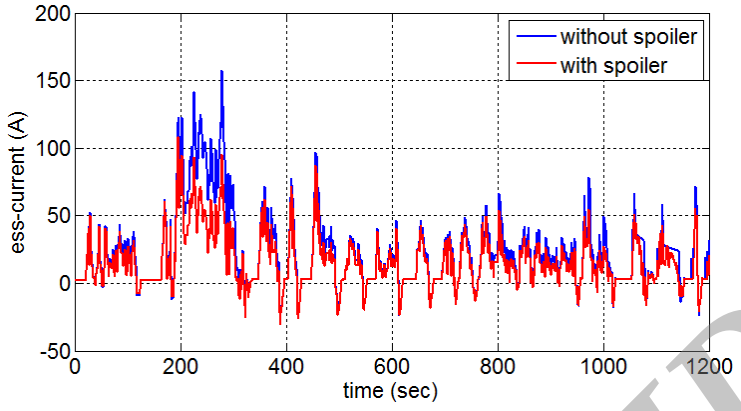

Fig. 17. Current output of the battery

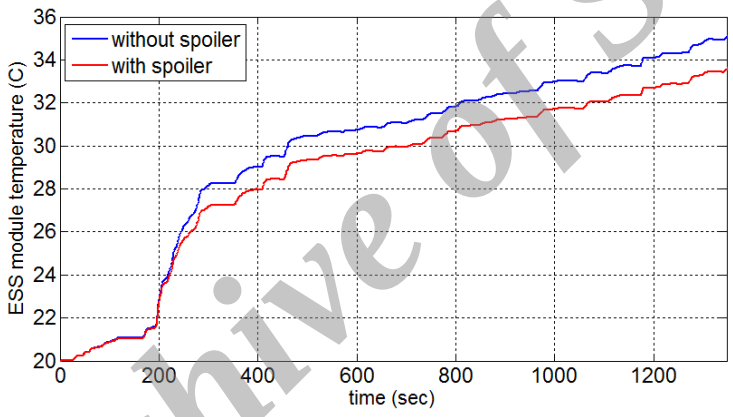

Fig 18. Temperature of battery module

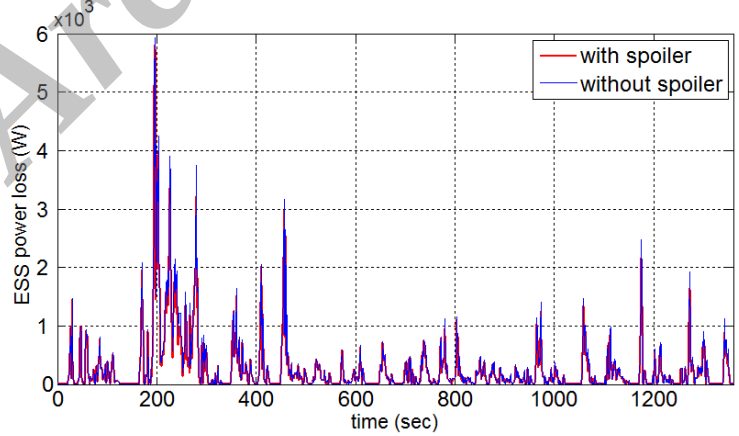

Fig 19. The actual power loss for the ESS

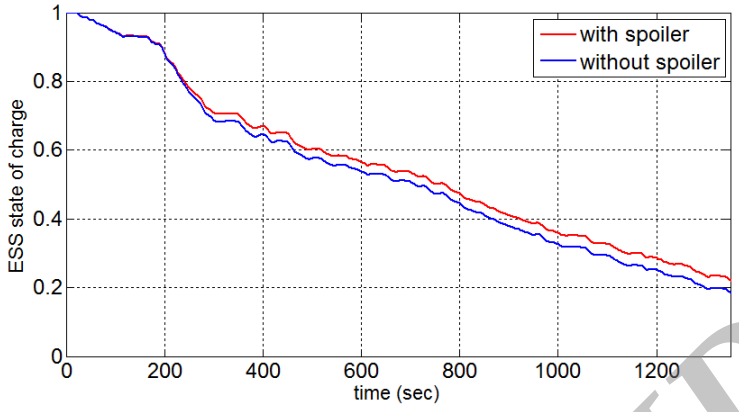

Fig 20. State of charge history

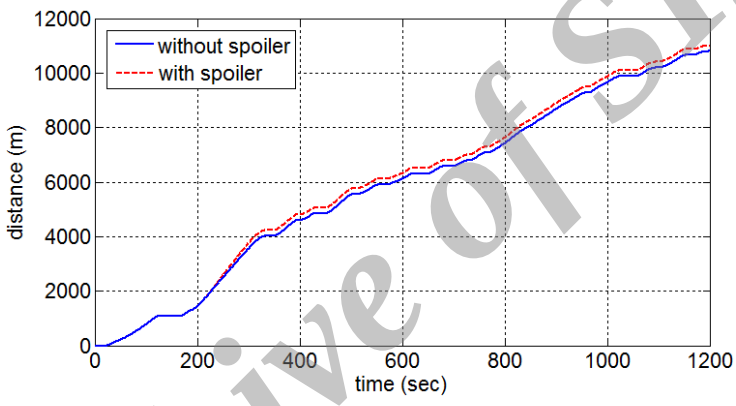

Fig 21. Time vector containing the distance the vehicle has traveled in case of UDDS Driving Schedule

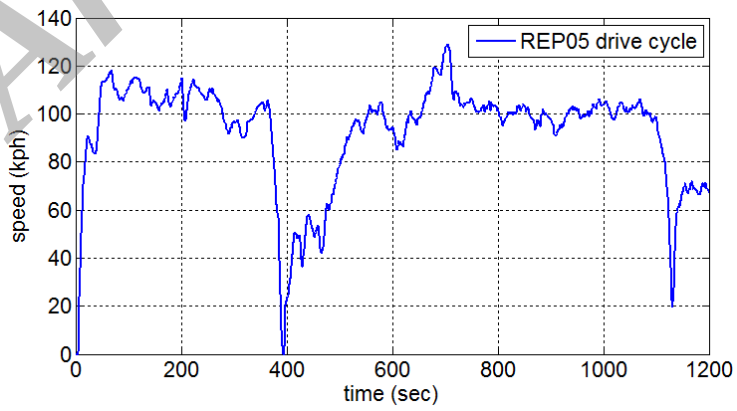

Fig 22. Requested vehicle speed for REP05 driving cycle

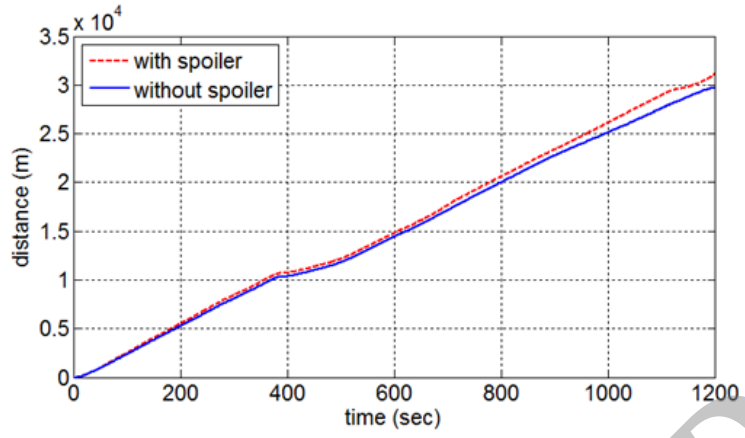

Fig 23. Time vector containing the distance the vehicle has traveled in case of REP05 Driving Schedule

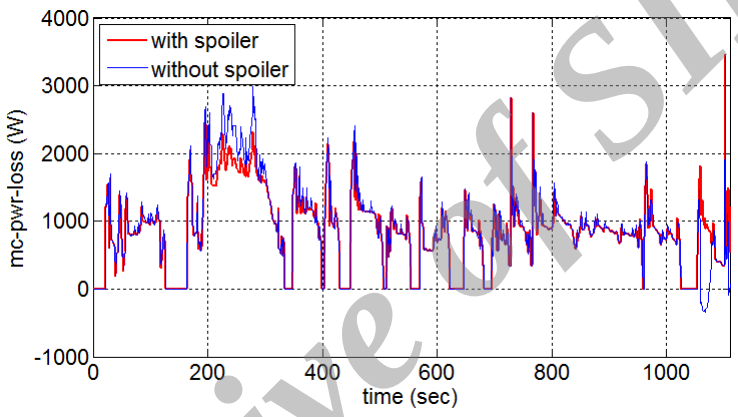

Fig 24. Power lost by BLDC motor

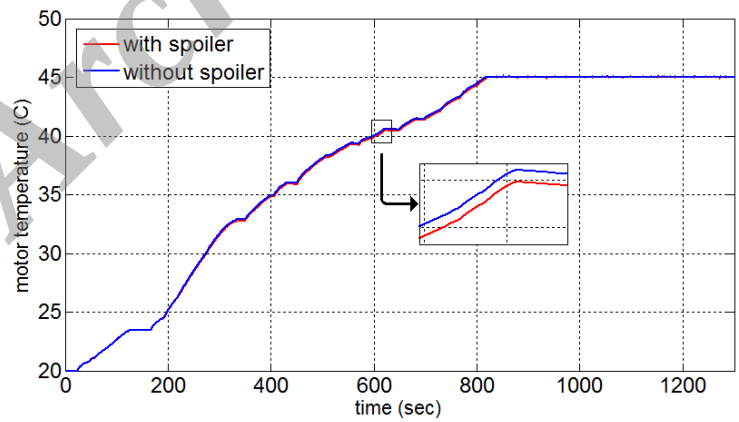

Fig 25. Temperature of motor

The traveling distances in two cases are also different. In order to compare the traveling distance in two cases, separate simulations were done in the same environmental condition. The results reveal that in case of an EV with spoiler the traveling distance is relatively more than traveling distance in case of no

spoiler installed (see Fig. 21). This shows that the spoiler is one of the necessities for maximizing the efficiency and distance travelled by EVs.

To further understand the effects of the spoiler on an electric vehicle mileage, a different driving cycle with higher driving speed, higher acceleration and deceleration need to be studied.

The Representative Drive Cycle Number 5 (REP05) was constructed from idle-to-idle segments of data that contained higher portions of speeds and accelerations than UDDS. This was intended to represent aggressive driving behavior. As illustrated in Fig. 22, this cycle can be split into three sections, the first segment has a highway aggressiveness factor of 0.64 m/s2 and this factor for the second segment of the cycle is 0.48 m/s2 [38]. The average speed in this drive cycle is 62 mph (100 kph), the maximum speed is 80.3 mph (129 kph), and the maximum acceleration rate is 8.5 mph/sec.as illustrated in Fig. 23 for this drive cycle, the difference of transferring mileage of electric vehicle with and without spoiler is obvious (2 km in 32km).

The decrease in current also reduces the power losses in electric motor and corresponding converters and drivers. According to Fig. 24 and Fig. 25, by install spoiler, more efficiency can be achieved in electric motor of EV.

As illustrated in equations (41) to (43), the BLDC motor efficiency depends on mechanical power and input power.

$$P_L = T_L . W_m \quad (41)$$

$$P_{in} = V_s . I_s \quad (42)$$

$$eff(\%) = \frac{P_L}{P_{in}} \times 100 \quad (43)$$

Where P_L the load is power on the motor shaft and P_{in} is the input power of the motor.

As shown in Figs. 26 and 27, ESS efficiency and BLDC efficiency affected by the aerodynamic effects because of variation of available output current from ESS.

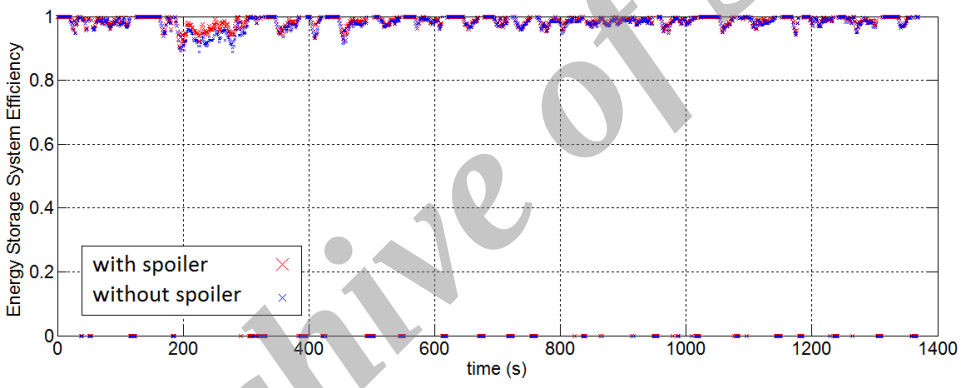

Fig 26. ESS efficiency map

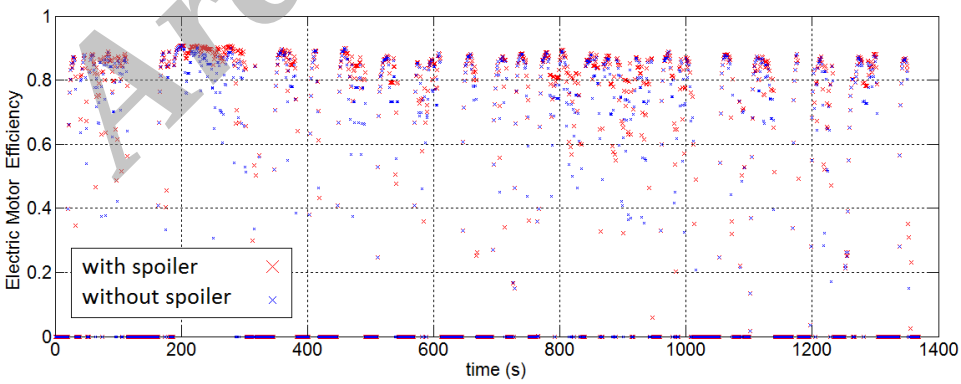

Fig 27. BLDC efficiency map

5. Experimental results

In these section practical and experimental results of evaluating the effects of installing a rear spoiler on an EV is presented. In this regard, an electric vehicle called Yoshita was designed and manufactured as shown in Fig. 28.

Driving force of this vehicle is supplied by a 10 kw brushless electric motor; also, energy storage system of this vehicle contains a set of sealed acid batteries (Hi-Ca model) with an output voltage of 72volts and also super capacitor modules (Maxwell model) with an output voltage of 48volts; Energy storage system of this vehicle is shown in Fig. 29.

Fig. 30 displays proposed spoiler manufactured as a result of this research which is installed on Yoshita EV. Parameters of presented system are regulated according to simulated parameters under the same conditions.

In order to investigate the experimental results under dynamic loading conditions and to create a proper background to compare experimental results, it is required that the considered EV which is equipped with/without a rear spoiler, become evaluated. This experiment should be conducted in a specific environment considering the standard driving cycle.

Hence, experiment on the provided EV has been conducted in the path shown in Fig. 31 and according to a specified speed displayed in Fig. 32, Speed is set automatically using Hall effect sensor (Honeywell S495A); required force in order to change the angle of Hall effect sensor is supplied by a set of digital servo motors (ALIGN DS610); in order to regulate required voltage of servo motors, voltage regulators (UBEC) are employed. In order to implement controller of the provided required speed, IC (8255A) is utilized.

According to a specified speed and path, current and voltage of battery are derived as in Figs. 33 and 34 when the proposed methods are/are not employed in practical test respectively. As it is evident in figures, output current of battery in two states of energy-going out (e.g. 0-25 seconds) and energy-returning in (e.g. 370-400 seconds) for regenerative braking case is close enough to the simulated results with an acceptable accuracy. Battery state of charge as a main factor in EVs is also sketched in Figs. 35 and 36 in first 400 second of standard driving cycles in a specified path when proposed methods are/are not employed respectively. As it is apparent by the figure, battery state of charge is ascending in particular moments, this happens when regenerative braking occurs. According to the Figs. 35 and 36, battery state of charge resulted from the practical test, guarantees simulation results.

Fig.28. Manufactured EV by authors of this paper

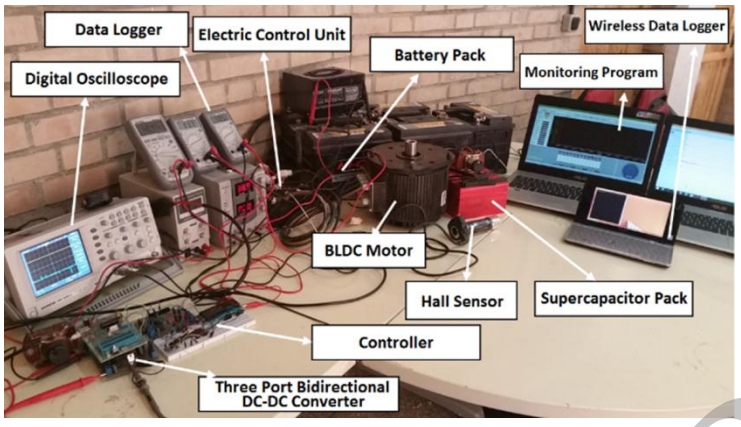

Fig.29. Energy storage system using in Yoshita EV

Fig.30. Proposed EV with the rear spoiler

Fig.31. Distance traveled in practical test

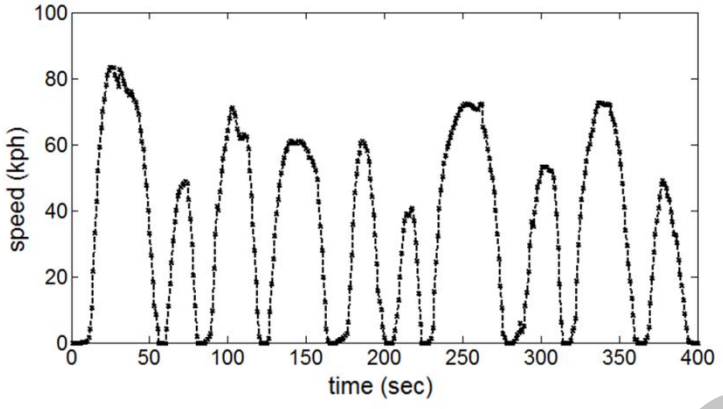

Fig 32. Speed of vehicle in practical test path

Fig.33. Battery voltage and current resulted from practical test by installing the rear spoiler

Fig.34. Battery voltage and current resulted from practical test by not installing the rear spoiler

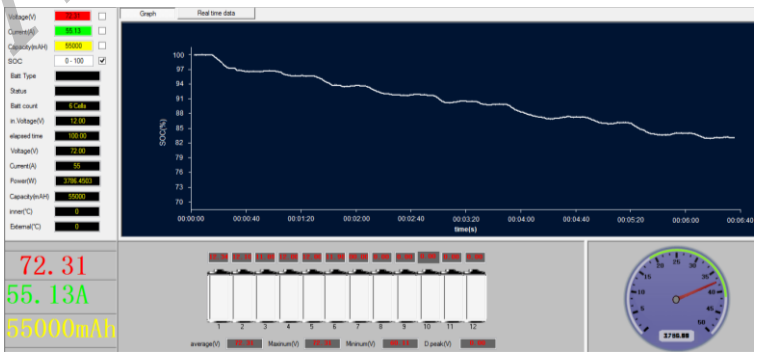

Fig.35. Battery state of charge resulted from practical test by installing the rear spoiler

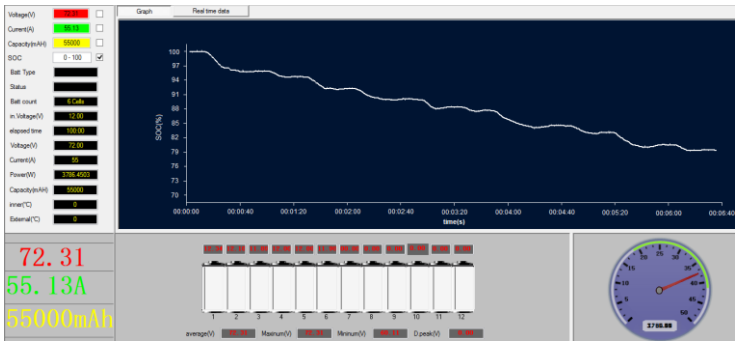

Fig.36. Battery state of charge resulted from practical test by not installing the rear spoiler

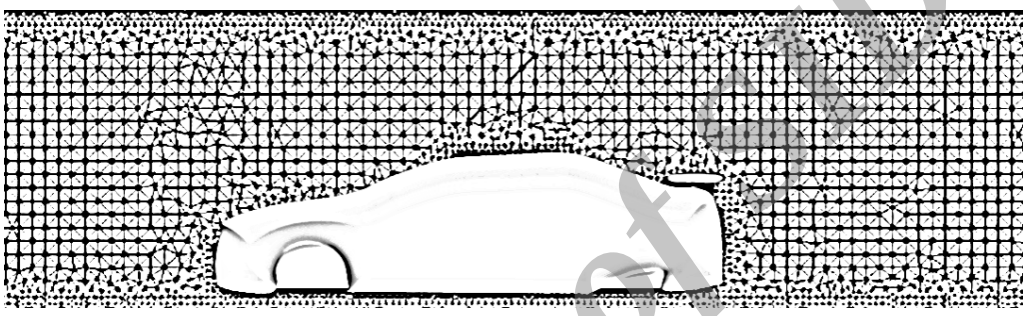

Fig. 37. Meshes generated around the proposed EV

Appendix I

Meshes generated around the body for proposed EV are illustrated in Fig. 2. The total number of the cells in the computational domain is about 1.5 million.

6. Conclusion

In this paper, the effects of installing a rear spoiler on performance of an EV were investigated through simulations and practical test. All components of an EV were modeled and it was shown that installing a rear spoiler reduced the drag coefficient up to 7 per cent which in turn reduced the energy consumption of vehicle. Furthermore, the lift coefficient decreased from 0.008 to -0.036. These reductions also entail another benefit which is the reduction of emission in ICE cars, but, in EVs the benefits are not limited just to abovementioned items. The reduction of drag and lift forces indirectly reduce the current drawn from batteries which leads to increasing the battery life, reducing the battery temperature and also power losses. In addition, it reduces the power losses in converters and electric motor. Consequently, the EV is able to travel more distances and keep more energy. Finally, the wheel slip of drive wheels reduces.

All in all, it can be concluded that the significant benefits obtained by installing rear spoiler on EVs make it a proper and inexpensive solution for improving the energy efficiency and performance of EVs.

References

[1]. N. Künzli, R. Kaiser, S. Medina and et al. "Public-health impact of outdoor and traffic-related air pollution: a European assessment", The Lancet, vol. 356, Issue 9232, pp. 795-801, Sept. 2000. [Online]. Available: http://dx.doi.org/10.1016/S0140-6736(00)02653-2.

[2]. R. C. Zake, "Aerodynamics of aftermarket rear spoiler", University Malaysia, Pahang, 2008.

[3]. D. P. Menon, S. Kamat, G. Yangnavalkya, S. Mukkamala and P. S. Kulkarni, "To improve the aerodynamic performance of a model hatchback car with the addition arear roof spoiler," 16th Annual CFD Symposium, 2014.

[4]. X. Hu, and T. T. Wong, "A Numerical Study On Rear-spoiler Of Passenger Vehicle", World Academy of Science, Engineering and Technology, International Science Index 57, vol. 5, pp. 514 - 519, 2011.

[5]. I. Kim, H. Chen and R. C. Shulze, "A Rear Spoiler of a New Type that Reduces the Aerodynamic Forces on a Mini-Van," SAE Technical Paper 2006-01-1631, 2006. [Online]. Available: http://dx.doi.org/10.4271/2006-01-1631.

[6]. Y. Kiyoshi, N. Hase, S. Fujita, R. Isomura, I. Takeda, K. Sumitani and T. Murayama., "Concurrent CFD Analysis for Development of Rear Spoiler for Hatchback Vehicles", Society of Automotive Engineers Inc, Warrendale, PA, 1997. [Online]. Available: http://dx.doi.org/10.4271/970410.

[7]. A. Parihar, A. Kulkarni, F. Stern, T. Xing and S. Moeykens, "Using FlowLab, an educational computational fluid dynamics tool, to performa comparative study of turbulence models", Computational Fluid Dynamics Journal, Vol. 15, No. 1, pp. 175-182, 2006.

[8]. Y. Takemori, S. Kato, Y. Masumitsu and T, Mizutani, "Drag Reduction of Bluff-Based by Wake Control Vanes(Effective Utilization of Under Floor Flow)", FISITA World Automotive Congress, F2000G357, 1992.

[9]. M. Kim, "Numerical Study on the Wake Flow and Rear-Spoiler Effect of a Commercial Bus Body," SAE Technical Paper 2003-01-1253, 2003. [Online]. Available: http://dx.doi.org/10.4271/2003-01-1253.

[10]. W. T. Mason and P. S. Beebe, "The Drag Related Flow Field Characteristics of Trucks and Buses", in Aerodynamics Drag Mechanism of Bluff Bodies and Road, Vehicle, Springer US, pp. 45-93, 1978. [Online]. Available: http://dx.doi.org/10.1007/978-1-4684-8434-2_3.

[11]. T. Fujimoto, A. Niinuma, K. Sakai, "Shape Study for a Low Air Resistance Air Deflector-The Second Report", SAE 950633, 1995. [Online]. Available: http://dx.doi.org/10.4271/950633.

[12]. K. P. Garry, "Development of Container Mounted Devices for Reducing Aerodynamic Drag of Commercial Vehicle", Journal of Wind Engineering and Industrial Aerodynamics, vol. 9, Issues 1–2, pp. 113–124, 1981. [Online]. Available: http://dx.doi.org/10.1016/0167-6105(81)90082-9.

[13]. A. Gilhaus and R. Hoffmann, "Directional Stability, Aerodynamics of Road Vehicles, in: W.H. Hucho (Ed.)", SAE International, Warrendale, PA, 1998.

[14]. J. R. Callister and A. R. George, "Measurement and Analysis of Automobile Wind Noise", SAE Technical Paper 930299, 1993. [Online]. Available: http://dx.doi.org/10.4271/930299.

[15]. F. R. Bailey and H. D. Simon, "Future Directions in Computing and CFD" , AIAA Paper 92-2734, 1992. [Online]. Available: http://dx.doi.org/10.2514/6.1992-2734

[16]. H. Taeyoung, V. Sumantran, C. Harris, T. Kuzmanov, M. Huebler and T. Zak, "Flow-field simulations of three simplified vehicle shapes and comparisons with experimental measurements", SAE Technical Paper 960678, pp. 820-835, 1996. [Online]. Available: http://dx.doi.org/10.4271/960678.

[17]. O. Baysal and I. Bayraktar, "Computational Simulation for External Aerodynamics of Heavy Trucks", SAE Technical Paper 2000-01-3501, 2000. [Online]. Available: http://dx.doi.org/10.4271/2000-01-3501.

[18]. J. Ferziger and M. Peric, "Computational Methods for Fluid Dynamics", 3rd ed, Springer, pp. 157-216, 2001. [Online]. Available: http://dx.doi.org/ 10.1007/978-3-642-56026-2.

[19]. T. N. Croft, "Unstructured mesh – finite volume algorithms for swirling, turbulent, reacting flows", Ph.D. thesis, University of Greenwich, 1998.

[20]. A. Dewan, "Tackling Turbulent Flows in Engineering", 1rd ed, Springer, Berlin, pp. 49-57, 2011. [Online]. Available: http://dx.doi.org/10.1007/978-3-642-14767-8.

[21]. D. Choudhury, "Introduction to the Renormalization Group Method and Turbulence Modeling", Technical Memorandum TM 107, Fluent Inc., Lebanon NH,pp. 1-30, 1993.

[22]. Bu-Ali Sine University (BASU) Solar Electric Vehicle. [Online]. Available: http://basuev.esy.es/

[23]. M. Ehsani, Y. Gao and A. Emadi, "Modern Electric, Hybrid Electric, and Fuel Cell Vehicles: Fundamentals, Theory, and Design", Second Edition, CRC Press, pp. 23-27, 2009.

[24]. R. Rajamani, "Vehicle dynamics and control", New York, NY: Springer, pp. 87-111, 2006. [Online]. Available: http://dx.doi.org/10.1007/978-1-4614-1433-9.

[25]. H. Dugoff, P. Fancher and L. Segel, "An analysis of tire traction properties and their influence on vehicle dynamic performance," SAE Technical Paper 700377, 1970. [Online]. Available: [Online]. Available: http://dx.doi.org/10.4271/700377.

[26]. A. Burke, "Batteries and ultracapacitors for electric, hybrid, and fuel cell vehicles," Proc. IEEE, vol. 95, no. 4, pp. 806–820, 2007. [Online]. Available: http://dx.doi.org/10.1109/JPROC.2007.892490.

[27]. A123 Systems. [Online]. Available: http://www.a123systems.com.

[28]. D. A. J. Rand, R. Woods and R. M. Dell, "Batteries for Electric Vehicles", Research Studies Press Ltd, pp. 125– 230, 1998.

[29]. S. M. Rezvanizaniani, Z. Liu, Yan Chen and J. Lee, "Review and recent advances in battery health monitoring and prognostics technologies for electric vehicle (EV) safety and mobility", Journal of Power Sources, vol. 256, pp. 110–124, 2014. [Online]. Available: http://dx.doi.org/10.1016/j.jpowsour.2014.01.085.

[30]. Y. H. Chiang, W. Y. Sean and J. C. Ke," Online estimation of internal resistance and open-circuit voltage of lithium-ion batteries in electric vehicles", Journal of Power Sources, Vol. 196, Issue. 8, pp. 3921-3932, [Online]. Available: http://dx.doi.org/10.1016/j.jpowsour.2011.01.005

[31]. H. He, R. Xiong and H. Guo," Online estimation of model parameters and state-of-charge of LiFePO4 batteries in electric vehicles", Journal of Apply Energy, Vol. 89, Issue 1, pp. 413–420, 2012. [Online]. Available: http://dx.doi.org/10.1016/j.apenergy.2011.08.005.

[32]. A. A. Pesaran, A. Vlahinos, and S. D. Burch, "Thermal performance of EV and HEV battery modules and packs," in Proceedings of the 14th Internal Electric Vehicle Symposium, Orlando, Fla, USA, 1997.

[33]. Z. Rao and S. Wang, "A review of power battery thermal energy management", Journal of Renewable and Sustainable Energy Reviews, vol. 15, pp. 4554– 4571, 2011. [Online]. Available: http://dx.doi.org/10.1016/j.rser.2011.07.096.

[34]. M. H. Moradi, S. M. R. Tousi, M. Nemati, N. Sadat Basir and N. Shalavi, "A Robust Hybrid Method for Maximum Power Point Tracking in Photovoltaic Systems", Journal of Solar Energy, vol. 94, pp. 266-276, 2013. [Online]. Available: http://dx.doi.org/10.1016/j.solener.2013.05.016.

[35]. S. Baldursson, "BLDC Motor Modelling and Control-A Matlab/Simulink Implementation", Goteborg, Sverige, 2005.

[36]. I. Husain," Electric and Hybrid Vehicles, Design Fundamental", CRC Press LLC, Florida, pp. 229-240, 2003.

[37]. T. Zackrisson, "Modeling and simulation of a driveline with an automatic gearbox", Master's thesis, Royal Institute of Technology, KTH, 2003.

[38]. B. I. Michelle, "The Effects of Driving Style and Vehicle Performance on the Real-World Fuel Consumption of U.S. Light-Duty Vehicles", Master's Thesis, Massachusetts Institute of Technology, 2010.

[39]. G. Leduc, "Longer and heavier vehicles, an overview of technical aspects", JRC Scientific and Technical Reports, European Communities, 2009.

[40].
[41]. S. Diamond, "Heavy Vehicle Systems optimization", Annual Progress Report for Heavy Vehicle Systems Optimization, Washington, D.C, U.S.A, 2004.
[42]. G. Genta and L. Morello, "The Automotive Chassis, Volume 1: Components Design" Netherlands, Springer, pp. 53-132, 2009. [Online]. Available: http://dx.doi.org/10.1007/978-1-4020-8676-2.
[43]. M. Amodeo, A. Ferrara, R. Terzaghi and C. Vecchio, "Wheel slip control via second-order sliding-mode generation", IEEE Transactions on Intelligent Transportation Systems, 11(1), pp.122–131, 2010. [Online]. Available: http://dx.doi.org/10.1109/TITS.2009.2035438.
[44]. S. M. Rezvanizaniani, Z. Liu, Y. Chen and J. Lee, "Review and recent advances in battery health monitoring and prognostics technologies for electric vehicle (EV) safety and mobility" Journal of Power Sources, vol. 256, pp.110-124, 2014. [Online]. Available: http://dx.doi.org/10.1016/j.jpowsour.2014.01.085.